Mission Performance Assessment of Multimode Propulsion for Satellite Servicing Applications

Giusy Falcone
Graduate Research Assistant, Aerospace Engineering
University of Illinois Urbana-Champaign
gfalcon2@illinois.edu

Daniel L. Engel
Graduate Research Assistant, Aerospace Engineering
University of Illinois Urbana-Champaign
dlengel2@illinois.edu

Marta Cortinovis
Undergraduate Research Assistant, Aerospace Engineering
University of Illinois Urbana-Champaign
martac2@illinois.edu

Charles N. Ryan
Lecturer in Astronautics
University of Southampton
c.n.ryan@soton.ac.uk

Joshua L. Rovey
Associate Professor, Aerospace Engineering
University of Illinois Urbana-Champaign
rovey@illinois.edu

Zachary R. Putnam
Assistant Professor, Aerospace Engineering
University of Illinois Urbana-Champaign
zputnam@illinois.edu

Steven Berg
Chief Executive Officer
Froberg Aerospace LLC
steven.berg@frobergaerospace.com

Michael Lembeck
Associate Professor of Practice, Aerospace Engineering
University of Illinois Urbana-Champaign
mlembeck@illinois.edu

***Abstract*— We assess the mission performance of a multimode (monopropellant-electrospray dual-mode) propulsion system relative to current state-of-the-art chemical, electric, and hybrid chemical-electric propulsion systems for satellite servicing applications. Performance is assessed for both low-Earth orbit servicers (with total mass of approximately 100 kg) and geosynchronous orbit servicers (with total mass of approximately 1000 kg). First-order spacecraft sizing routines are developed to determine spacecraft properties for each propulsion system option based on historical data, propulsion system properties, and physical and geometric constraints. The overall servicing missions are decomposed into a set of discrete maneuvers for both servicer concepts. Simulations are developed for each maneuver and propulsion system to determine flight performance, including ΔV and time of flight.**

Finally, metrics of comparison between the different propulsion system options are proposed to illustrate the strengths and weaknesses of each propulsion system option over the candidate mission scenarios. Mission scenarios are composed of admissible sequences of modeled maneuvers. Comparison metrics are then used to highlight the costs and benefits of the assessed propulsion system options relative to each other. Results indicate that the hybrid and multimode systems provide significant mission flexibility for satellite servicing applications, but the multimode does so with a significantly lower structural ratio.

TABLE OF CONTENTS

978-1-6654-3760-8/22/$31.00 ©2022 IEEE

1. INTRODUCTION

Future servicing satellites may provide robotic assistance to a client constellation. On-orbit servicing interest has increased in the past five years due to its potential to extend mission lifetime [1] by providing a wide range of capabilities, such as orbit modification and maintenance, propellant resupply, repairing clients, and orbital debris mitigation [2]. Servicing satellites may be equipped with different propulsion systems, such as, chemical, electric, hybrid and multimode. An exclusively high-thrust chemical propulsion system enables timely, but propellant intensive maneuvers, avoiding long spiral trajectories typical of electric propulsion system maneuvers. High-specific impulse electric propulsion, although time intensive, saves propellant compared to a chemical thruster, increasing mission lifetime and maneuver capability [3]. Hybrid and multimode propulsion enable the use of both chemical and electric propulsion modes on a spacecraft. A multimode servicer is a servicer equipped with a single propulsion system, which feeds both chemical and electric electrospray thrusters with shared propellant [4]. The hybrid concept uses independent propulsion systems to provide different types of propulsive modes. Unlike hybrid propulsion, preliminary allocation of propellant to a specific mode of operation is not required in multimode propulsion, offering mission designers a choice between high-thrust chemical propulsion, or high-efficiency electric propulsion on demand throughout an entire mission [3].

The multimode propulsion investigated is a "one-size-fits-most" space propulsion system that feeds shared propellant to both a chemical catalyst decomposition thruster and an electrospray thruster. The dual-mode propellant implemented consists of a blend of 1-ethyl-3-methylimidazolium ethyl sulfate ([Emin][$EtSO_4$]) and hydroxylammonium nitrate (HAN), also known as FAM-110A (Froberg Aerospace Multimode Propellant 100A)[4]. Berg and Rovey's recent work [5] has demonstrated stable sub-scale single emitter electrospray operation, along with catalytic ignition and long duration decomposition in chemical microthruster of FAM-110A. This system can meet needs across many different mission scenarios, providing a high-thrust chemical mode and a high efficiency electrospray mode with performance

comparable to state-of-the-art propulsion systems. Previous assessment of the application of the system to a 6U-sized CubeSat demonstrated that multimode propulsion provided the highest mission ΔV capability for missions lasting less than 150 days compared to state-of-the-art propulsion systems employing other modes [3].

The performance of multimode propulsion systems in a mission design context has not been extensively studied in the literature. A satellite servicing vehicle with a multimode system on-board theoretically offers flexibility for the mission design in that the single servicing vehicle can perform both low- and high-thrust maneuvers without any pre-allocation of propellant to a particular system. Hence, maneuvers can be modified or added both prior to launch and during the mission to accommodate time and propellant mass constraints. To accurately gauge flexibility and performance benefits provided by a multimode system relative to existing propulsion system options, mission analysis must be performed, and flight performance must be assessed.

In this investigation, multimode propulsion systems were analyzed for Geosynchronous orbit (GEO) servicers and low-Earth orbit (LEO). The GEO servicers are assumed to loiter in the geosynchronous graveyard orbit (GYO), 300 km above the client in GEO. The GEO servicer mission is composed of a sequence of maneuvers including orbit lowering and phasing, rendezvous with a client in GEO, relocation of a GEO client to a different GEO slot, disposal of GEO client to GYO, mass transfer to a client, investigation of a client, and return to GYO. The LEO servicers are instead assumed to loiter in a perch orbit 50 km above the client LEO orbit. The LEO servicer mission is composed of the same sequences as the GEO servicer, such as lowering and phasing, rendezvous with a client in LEO, relocation of a LEO client to a different LEO slot, disposal of client, mass transfer to a client, investigation of a client, and return to perch. For LEO cases, disposal of a client is achieved by releasing the client into a 25-year orbit.

In this study, schemes were developed to size multimode (MM) propulsion system for LEO and GEO servicers. Chemical (chem), electric (elec), and hybrid (hyb) systems were also sized for comparison to the multimode system. A set of maneuvers including orbit raising, lowering, and phasing were defined and assessed for the LEO and GEO servicers, with different propulsion system options and methods for executing the maneuvers using mission analysis software. Both the sizing and mission analysis were used to characterize the system on several levels, including mission performance, complexity, cost, and resiliency.

2. SPACECRAFT AND PROPULSION SYSTEM SIZING

Sizing routines were developed to determine vehicle properties for the LEO and GEO servicers for each propulsion mode: chemical, electric, multimode, and hybrid. The single-mode chemical system included a hydrazine monopropellant thruster, the single-mode electric system employed a Hall-effect thruster utilizing Xenon propellant, while the hybrid system equipped both technologies. Once again, the multimode system is comprised of a monopropellant-electrospray thruster, using FAM-110A as the shared propellant. All systems were compared on the basis of thrust, specific impulse, and system mass. Performance of all systems applied to LEO and GEO servicers was characterized by time and propellant utilized to perform a specified maneuver, as well as the remaining maneuver capability throughout the entire mission. For all vehicle types, the propulsion system wet mass was assumed to be a fixed percentage of the total spacecraft mass. The total spacecraft mass was constant for the LEO and GEO vehicles respectively, regardless of propulsion system type. Propulsion systems were iteratively sized to maintain consistent total spacecraft mass while maximizing the propellant mass available.

Propulsion System Sizing

The sizing procedure begins with an initial guess for the propellant mass. The total propellant mass of the hybrid system was divided in half and allocated to the chemical and electric systems respectively. To account for unusable residual propellant, an additional 5% of the initial propellant mass was added. Using the propellant density, the volume of the propellant was calculated. Propellant densities, as well as operating pressures are provided in Table 1. 10% of calculated tank volume was added to account for ullage. The propellant tanks are assumed to be spherical titanium tanks with a density of 4430 kg/m^3 and a tensile strength $\sigma = 83000$ kPa [6]. The thickness of the spherical shell propellant tank can be approximated by [7]

$$t = \frac{P_b r}{2\sigma} \tag{1}$$

where t is the tank thickness, r is the inner radius of the tank, and P_b is the burst pressure, which is assumed to be 1.25 times the operating pressure [3]. With the thickness of the propellant tank known, tank mass can be estimated.

Table 1: Propellant Densities and Operating Pressures

Propellant	Density (kg/m^3)	Operating Pressure (kPa)
Hydrazine	1000 [8]	37700 [9]
Xenon	1642 [3]	110000 [3]
FAM-110A	1420	30000

The mass of the helium pressurant is calculated using:

$$m = \frac{P_p V_p}{R T_i} \left(\frac{K}{1 - \frac{P_g}{P_i}} \right) \tag{2}$$

where m is the mass of the helium pressurant, P_p is the instantaneous pressurant pressure in the propulsion tank, V_p is the instantaneous pressurant volume in the propulsion tank, R is the specific gas constant (2077.3 J/kg-K), T_i is the initial pressurant temperature (300 K), K is the ratio of specific heats (1.67), P_g is the instantaneous pressurant pressure in the pressurant tank, and P_i is the initial pressurant pressure in the pressurant tank (14000 kPa). With a pressurant mass known, the density and volume of helium at maximum tank pressure can be calculated through the ideal gas law (compressibility factor of 1.0). As with the propellant tank volume, 10% of the volume is added to account for ullage. The pressurant tank thickness is then calculated like the propellant tank using Eq. (1). Note that the hybrid servicers have two pressurant tanks—one for the chemical system and one for the electric system, while the other propulsion systems have a single pressurant tank.

Known masses of similar thrusters were used to approximate the dry mass of the thrusters for the different propulsion

system options. Propellant lines and valves is assumed to be half the mass of the thruster(s), and mounting hardware is assumed to be 10% of the inert propulsion system mass [3]. The inert mass includes thrusters, lines/valves, propellant and pressurant tanks, mounting hardware, and a power processing unit (PPU) if applicable.

LEO Servicer Sizing

The above procedure was used to size propulsion systems for several LEO servicers: multimode, chemical, electric, and hybrid. For an equal comparison among all four vehicle options, the propulsion system wet mass was assumed to be 30% of the total spacecraft wet mass (100 kg). The other spacecraft subsystems mass were defined following Ref. [10]. Results for this sizing process are given in Table 2. The component masses in Table 3 were used to generate these sizing results. According to Table 2, the multimode system allows for the second-highest propellant mass of the considered systems; the multimode propellant mass is 2.87 kg lower than the chemical system, and 3.88 kg greater than the hybrid system. The multimode system also allows for a significantly lower propulsion system dry mass than both the electric system and hybrid system. Part of this is due to the commonality of the multimode system. A metric for the commonality of the multimode system is the system integration factor, f_{SI} [3]:

$$f_{\text{SI}} = 1 - \frac{m_{\text{int}}}{m_{\text{sep}}} \tag{3}$$

where m_{int} is the dry mass of the integrated propulsion system (i.e. multimode), and m_{sep} is the dry mass of the separate propulsion system (i.e. hybrid). Carrying out this calculation yields a system integration factor of 0.36 for the LEO servicer concept. Another factor contributing to the larger dry mass of the electric and hybrid system is the high operating pressure of the xenon propellant, which requires a large and thick pressurant tank. This is further highlighted by the pressurant tank radii in Table 2, in which the radius for the electric pressurant tank is 1.63 times the radius of the multimode pressurant tank. The multimode system also outperforms the hybrid system from a volume perspective. For both the propellant and pressurant tanks, the single-tank multimode system has a radius of similar order of magnitude to the radii of the dual-tanks of hybrid system. In Table 2 for the hybrid system, the "C" indicates the tank for the chemical system, the "E" indicates the tank for the electric system, and the "S" indicates components that may be shared between the two systems (e.g. propellant feed lines and mounting hardware). Hence, the multimode system can accommodate a larger propellant mass and operate with smaller tanks, while also using a lower propulsion system dry mass, relative to the hybrid and electric systems.

In addition to determining the mass and radii of propulsion system elements, the propulsion system sizing process also involved determining thruster properties for the different propulsion system options. For both low-thrust/electric and high-thrust/chemical modes, specific impulse values (I_{sp}) were chosen from those representative of the current state-of-the-art [4][11]. The thrust values for high-thrust/chemical modes were linearally scaled from a 6U cubesat concept and were assumed to be the same value for all vehicle options. To determine the thrust for each of the low-thrust/electric modes, the thrust was related to the propulsion system input power

Table 2: LEO Servicer Propulsion Systems

	Chem	**Elec**	**MM**	**Hyb**
Propellant Mass (kg)	26.21	8.84	23.34	19.46
Propulsion System Dry Mass (kg)	3.56	10.66	6.55	1.46(C) 6.82 (E) 1.92 (S)
Propellant Tank Radius (m)	0.19	0.14	0.16	0.14 (C) 0.12 (E)
Pressurant Tank Radius (m)	0.14	0.18	0.11	0.10 (C) 0.15 (E)

Table 3: Component Masses for LEO Servicer Systems

	Chem	**Elec**	**MM**	**Hyb**
Chemical Thruster Mass (kg)	0.60 [11]	-	0.86	0.60
Electric Thruster Mass (kg)	-	1.20 [11]	0.13	1.20
PPU Mass (kg)	-	3.30 [12]	3.30	3.30

using:

$$T = 2\eta \left(\frac{P}{I_{sp} * g_0} \right) \tag{4}$$

Here, T is the thrust, P is the propulsion system input power, g_0 is the acceleration due to gravity at Earth, and η is the thruster efficiency. The input power and efficiency were assumed for each system based on similar classes of propulsion systems [11], allowing the thrust for each system to be computed. A summary of the propulsion system properties for the LEO system is provided in Table 4.

Table 4: LEO Servicer Thruster Properties

	Chem	**Elec**	**MM**	**Hyb**
High Thrust (N)	12.82	-	12.82	12.82
Low Thrust (mN)	-	3.06	7.14	4.08
High Isp (s)	-	2000	1000	1500
Low Isp (s)	250	-	226	230
Power (w)	-	100	100	100
Efficiency	-	0.3	0.35	0.3

GEO Servicer Sizing

A similar procedure was used to size propulsion systems for the GEO servicers: multimode, chemical, electric, and hybrid. For the GEO servicers, however, sizing of spacecraft subsystems was carried out using a statistical design model approach, which used a database of 462 geostationary Earth orbit communication satellites launched from 2000 to 2017 and provided percentages of each spacecraft subsystem with

respect to the dry mass [13]. Additionally, the power subsystem mass and the solar panels of the chemical servicer were sized to generate a lower amount of power compared to the other servicers' options, due to their lower power requirements. Overall, this analysis resulted in a propulsion system wet mass approximately equal to 47% of the total spacecraft wet mass (1000 kg) for multimode, electric, and hybrid and a propulsion system wet mass approximately equal to 61.4% of the total spacecraft wet mass for the chemical servicer [10]. Results for this sizing process are given in Table 5. The component masses in Table 6 were used to generate these sizing results.

The results in Table 5 show that for the GEO vehicles, the multimode system provides the second-largest available propellant mass, as well as the lowest propulsion system dry mass. In particular, the multimode propellant system dry mass is 48.55 kg lower than the hybrid servicer, which allows for a larger propellant mass. As with the LEO servicer, the multimode system gets performance enhancements over the hybrid system due to hardware commonality. For the GEO multimode servicer, the system integration factor is 0.61. Additionally, the operating pressure of the FAM-110A utilized on the multimode system is the lowest of all the considered propulsion systems. The lower pressure allows for a pressurant tank that is thinner, smaller and less massive, relative to the electric and hybrid systems, thus the electric pressurant tank has a radius 1.68 times that of the multimode system. Furthermore, the hybrid system has two pressurization tanks: one that is 0.95 times the radius of the multimode tank and one that is 1.37 times the radius of the multimode tank. The use of these larger tanks not only contributes to a larger propulsion system dry mass but also may require the spacecraft to be larger in size.

Table 5: GEO Servicer Propulsion Systems

	Chem	Elec	MM	Hyb
Propellant Mass (kg)	556.38	356.43	435.98	382.62
Propulsion System Dry Mass (kg)	52.48	103.58	31.66	80.21
Propellant Tank Radius (m)	0.53	0.39	0.43	0.37 (C) 0.31 (E)
Pressurant Tank Radius (m)	0.29	0.48	0.285	0.27 (C) 0.39 (E)

Table 6: Component Masses for GEO Servicer Systems

	Chem	Elec	MM	Hyb
Chemical Thruster Mass (kg)	1.00 [11]	-	1.00	1.00
Electric Thruster Mass (kg)	-	3.30 [11]	1.90	3.30
PPU Mass (kg)	-	3.30 [12]	3.30	3.30

The GEO servicer thruster properties were determined using the same procedure utilized for the LEO servicer. A summary of the propulsion system properties for the GEO system is provided in Table 7.

Table 7: GEO Servicer Thruster Properties

	Chem	Elec	MM	Hyb
High Thrust (N)	128.21	-	128.21	128.21
Low Thrust (mN)	-	32.11	49.95	43.81
High Isp (s)	-	2000	1000	1500
Low Isp (s)	250	-	226	230
Power (w)	-	700	700	700
Efficiency	-	0.45	0.35	0.45

3. MANEUVER MODELING AND PERFORMANCE

The General Mission Analysis Tool (GMAT) [14] was used to model a set of likely maneuvers of the different servicing vehicles. The capabilities of GMAT allow for orbit propagation and for determining the necessary maneuver time and ΔV for a given maneuver. For this study, the force model in GMAT utilizes two-body orbital dynamics without additional perturbations for all the maneuvers other than station keeping. The station keeping maneuver considers the effect of atmospheric drag, gravitational perturbations, and the presence of Moon and Sun. All propulsive maneuvers are modeled as finite burns.

The maneuvers considered for analysis include phasing to or with a client, station keeping, raising to a graveyard orbit for the GEO servicer; phasing to or with a client, station keeping, and raising to a perch orbit for the LEO servicer. Full servicer missions may then be constructed with combinations of these maneuvers.

GEO Maneuver Modeling

The GEO scenarios involve a client in GEO (35786 km altitude, circular orbit) with a 0.05 deg inclination. The servicer is initially in GYO, a circular orbit 300 km above the client orbit (GEO). Maneuvers of interest include the servicer lowering and raising its orbit between the client and GYO, as well as changing phase with the client. A combined phasing and orbit raise/lower can also be performed.

Orbit Raising and Lowering

One of the assessed maneuvers, known as the "GYO raise" involves the servicer raising itself (or a combination of itself and the client for disposal) from the client's orbit to GYO. The same maneuver can be performed to lower the orbit from GYO to the client's orbit. For high-thrust chemical systems, this maneuver is composed of two finite burns in a near Hohmann transfer to conserve propellant. The first ΔV occurs near periapsis to raise the apoapsis, and the second ΔV occurs near the new apoapsis to raise the periapsis. The GMAT differential corrector solves for the length of the two thrust arcs, as well as the time between them, necessary to reach GYO. The thrust vector is assumed to be parallel to the inertial velocity vector during the two maneuvers. A diagram of the GYO lower using a high-thrust mode is shown in Fig. 1.

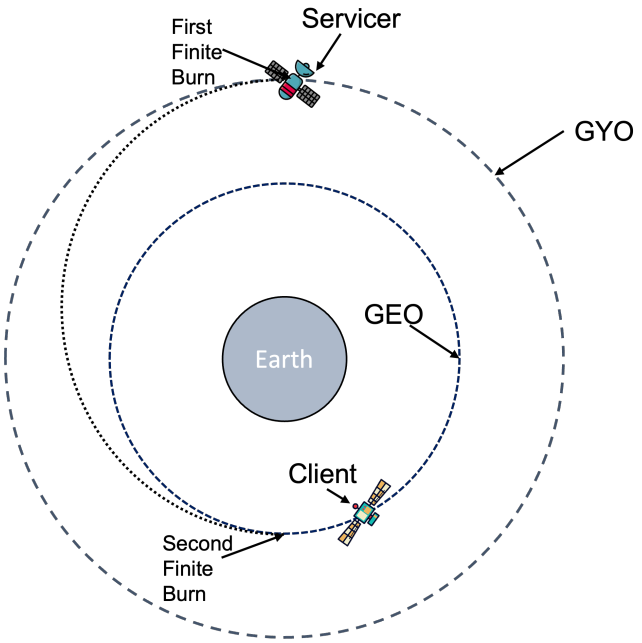

Figure 1: GYO lower with high-thrust mode.

For low-thrust electric systems, a continuous-thrust spiral maneuver is performed, where the orbit altitude slowly increases over many revolutions about the Earth. Like the low-thrust maneuvers, the thrust is maintained parallel to the local velocity vector while in operation. The trajectory is propagated until the semimajor axis approaches the desired value. A diagram of the GYO lower using a low-thrust mode is shown in Fig. 2.

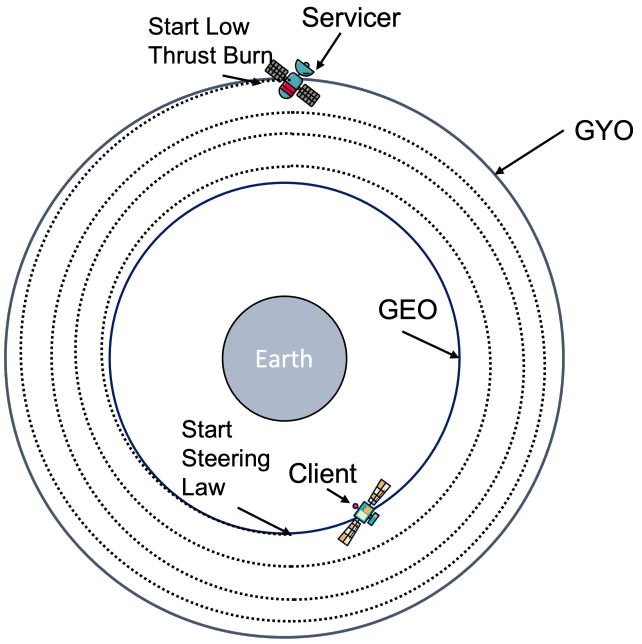

Figure 2: GYO lower with low-thrust mode.

The authors found that when operating in GEO, where the gravity from Earth is relatively low, and the orbital period is relatively large, a continuous low-thrust perturbs the orbit, resulting in oscillations in the orbital altitude and a non-zero eccentricity. If no corrective action is taken as the servicer raises its semimajor axis, the orbit radius will oscillate about the semimajor axis and the resultant orbit (GYO), as shown in Fig. 3. The GYO altitude corresponds to the target radius, shown as a dashed black line in the plot.

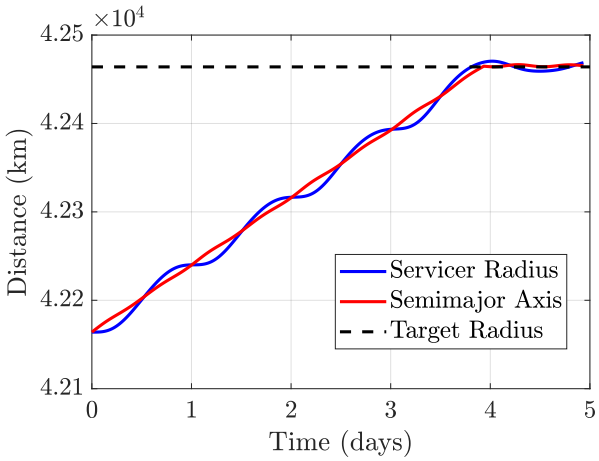

Figure 3: Orbital radius and semimajor axis as a function of time for GYO raise when no steering is used.

To circularize the orbit, an alternative raising procedure can be performed. First, the servicer uses the low-thrust mode as described earlier to raise its orbit until the apoapsis altitude is equal to the GYO semimajor axis. At this point, the servicer is in an elliptical orbit with a semimajor axis lower than the GYO semimajor axis. To circularize the orbit while also continuing to raise the semimajor axis, steering is performed (i.e. the thrust is no longer always parallel to the velocity vector). A steering law from Ref. [15], originally utilized for transferring from geosynchronous transfer orbit to GEO, was adapted to perform this circularization. The steering law works by only applying thrust in a certain range of true anomaly values (θ) near apoapsis. For this analysis, a range of 150-210 deg was found to provide good performance. While in this true anomaly range, the thrust angle α between the negative thrust direction and velocity vector is [15]:

$$\alpha = \tan^{-1}\left(Y\left[1 - e\sin\frac{\theta}{2}\sin\frac{\theta}{2}\right]\right) \tag{5}$$

Where, e is the eccentricity and Y is given by:

$$Y = -2\frac{\cot(0.5\theta)}{1 + e\cos\theta} \tag{6}$$

This steering law allows for the GYO semimajor axis to be achieved in the low-thrust modes, with very little oscillations in the orbit radius. A plot of radius and semimajor axis over time when the steering law is utilized is shown in Fig. 4. In this example, two revolutions are required to circularize the orbit once the desired apoapsis has been reached. The steering profile used during each of these circularization maneuvers is given in Fig. 5.

Results for performing the GYO raise with various propulsion system options are shown in Tables 8 and 9. These tables provide the utilized propellant, time the thruster is in operation, total maneuver time, and ΔV required for each of the

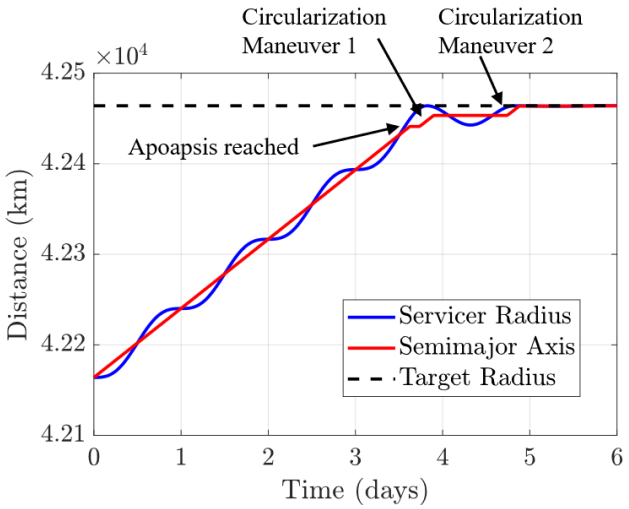

Figure 4: Orbital radius and semimajor axis as a function of time for GYO raise when steering is used.

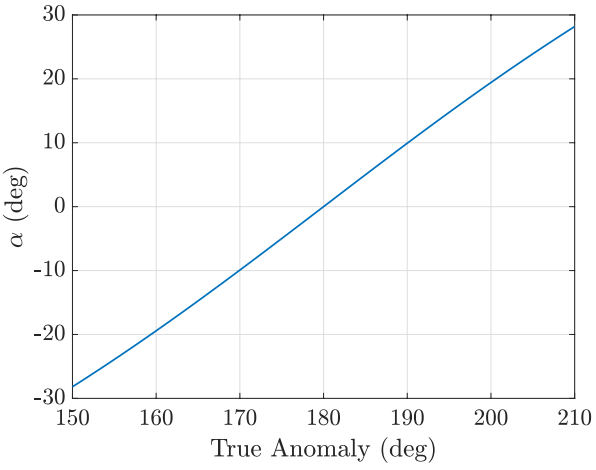

Figure 5: Steering profile used during circularization.

considered propulsion system options for a servicer undergoing the GYO raise maneuver. Table 8 shows the results for the GYO raise maneuver without carrying the client, while Table 9 shows the same maneuver when the servicer carries the client. Generally, results of the GYO raise maneuver with client (Table 9) requires larger propellant mass for all the propulsive system options and longer maneuvers for the low-thurst propulsive system options. This effect is due to the large client mass (2500 kg), which is 2.5 times larger than the initial servicer total mass.

Among the high-thrust systems in Tables 8 and 9, the chemical system utilizes the least amount of propellant, while the multimode utilizes the most propellant. For low-thrust options, the electric system utilizes the least propellant, and the multimode system utilizes the most propellant. Propellant expended is related to the specific impulse of a propulsion system, of which the multimode system has the lowest values relative to the other propulsion system options. The thruster on time is essentially the same for all high-thrust options also between the two different maneuvers, but differs for low-thrust, as the time taken to complete the maneuver depends

Table 8: GEO Servicer GYO Raise Performance

Propulsion Mode	**Propellant Used**	**Thruster On Time**	**Maneuver Time**	ΔV
Chemical	4.427 kg	84.67 s	0.5 days	10.90 m/s
Electric	0.556 kg	3.93 days	4.89 days	10.91 m/s
Multimode High-Thrust	4.9 kg	84.65 s	0.5 days	10.90 m/s
Multimode Low-Thrust	1.12 kg	2.54 days	3.67 days	10.98 m/s
Hybrid High-Thrust	4.81 kg	84.65 s	0.5 days	10.90 m/s
Hybrid Low-Thrust	0.74 kg	2.95 days	3.9 days	10.91 m/s

Table 9: GEO Servicer GYO Raise Performance with Client

Propulsion Mode	**Propellant Used**	**Thruster On Time**	**Maneuver Time**	ΔV
Chemical	15.49 kg	296.36 s	0.5 days	10.88 m/s
Electric	1.94 kg	13.72 days	14.8 days	10.88 m/s
Multimode High-Thrust	17.13 kg	296.2s	0.5 days	10.88 m/s
Multimode Low-Thrust	3.88 kg	8.23 days	9.85 days	10.88 m/s
Hybrid High-Thrust	16.84 kg	296.3 s	0.5 days	10.88 m/s
Hybrid Low-Thrust	2.56 kg	10.16 days	10.16 days	10.8 m/s

on the thrust value a particular system can produce and the total mass of the system. As the total mass increases, the maneuver time increases. Also, as the thrust increases, the maneuver time decreases. The multimode system has the largest electric thrust value among the considered systems, resulting in the shortest thruster operation time.

Phasing Maneuver

The phasing maneuver involves a change in the time-position of the servicer relative to the client. In the considered scenario, it is assumed that a phasing maneuver is performed to rendezvous with a client or to relocate a client in GEO. As with the GYO raise, the method for performing the phasing maneuver changes depending on the thrust mode used. In the case of the high-thrust mode, the phasing maneuver consists of two finite burns. The first ΔV places the servicer on an intermediate orbit that increases the servicer's orbital period, which modifies the orbital speed of the servicer relative to the client. The second ΔV is performed at the original maneuver point when the true anomaly of the servicer and the client approximately coincide. This second ΔV re-circularizes the servicer's orbit. The servicer can also maintain the intermediate orbit between two smaller magnitude maneuvers for a fixed amount of time to decrease the required propellant. Longer coasting time on the intermediate orbit results in lower overall propellant required for a given phasing maneuver. Fixing the number of coasting orbits allows the calculation of the intermediate orbit semimajor axis. For GEO orbits, the number of coasting orbits is fixed to 15. The GMAT differential corrector estimates the length of the two thrust arcs required to first modify the semimajor axis and then circularize the orbit. The thrust vector is kept parallel to the inertial velocity vector for both maneuvers, however, their direction is opposite to each other. A diagram showing the phasing maneuver using a high-thrust mode is shown in Fig. 6.

In the low-thurst mode, the phasing maneuver consists of spiraling up (or down) for a fixed amount of time and spi-

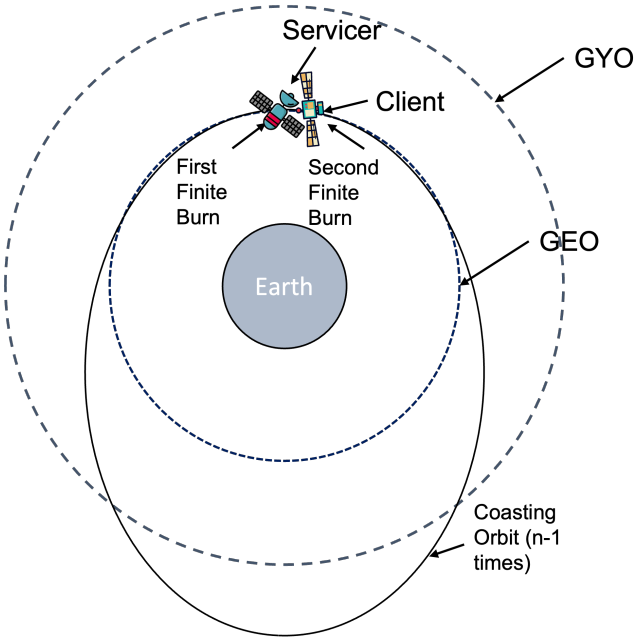

Figure 6: Phasing maneuver using high-thrust mode.

raling down (or up) for approximately the same time. In this case, the problem requires finding the minimum thruster on time to equal out the phasing angle between the servicer and the client. GMAT is used to define how the phasing angle changes in time; these results are then interpolated to estimate an initial guess for the thruster on time, as shown in Fig. 7. The two maneuvers are initially considered equal, although the thrust directions for the two maneuvers are opposite each other. Finally, the propagator uses the initial guess to perform the complete maneuver, which cancels out the phasing angle difference and also allows the vehicle(s) to reach the original orbit altitude and eccentricity. A diagram showing the phasing maneuver using a low-thrust mode is shown in Fig. 8.

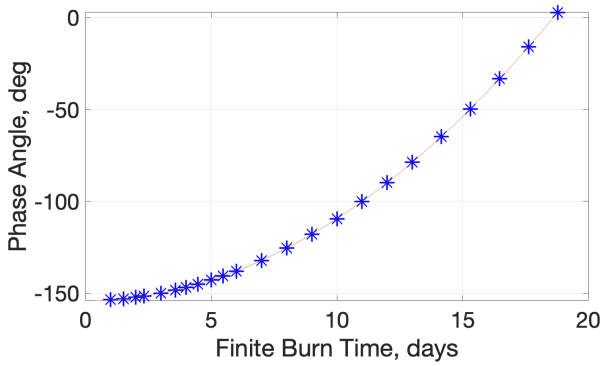

Figure 7: Phase angle variations with respect to the thruster on time.

Analogous to the high-thrust mode, this phasing maneuver can introduce a coast time to decrease the required propellant. In this case, the thrust-coast-thrust maneuver summarizes as follows: the phasing angle is defined as the sum between the phasing angle compensated through thrusting and the phasing angle compensated through coasting ($\phi = \phi_{thrust} + \phi_{coast}$). Thus, one of two angles is fixed, and the initial guess for

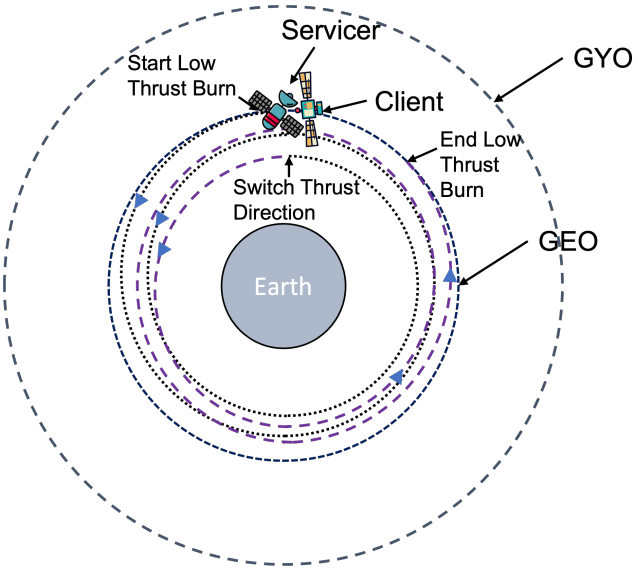

Figure 8: Phasing maneuver using low-thrust mode.

the maneuver is defined as before, while the coasting time is defined as:

$$\Delta t_{coast} = \Delta\phi_{coast} / \left(\dot{\nu}_{client} - \dot{\nu}_{servicer}\right) \tag{7}$$

where Δt_{coast} is the coasting time, $\Delta\phi_{coast}$ is the phasing angle compensated through coasting, and $\dot{\nu}$ is the time rate of change of the true anomaly angle. Also in this case, the propagator uses both initial guesses (thruster on time and coasting time) to perform the complete maneuver.

Figure 9 shows the propellant mass variation with respect to the maneuver time for a 90 deg phasing angle maneuver. The total maneuver time is the sum of the thruster on time and the coast time. As visible from the plot, increasing the maneuver time results in a decrease in the propellant used.

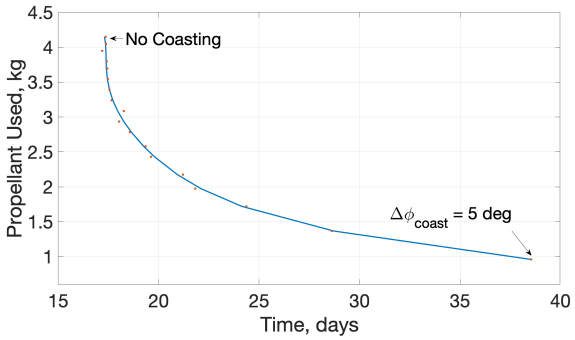

Figure 9: Phase angle variations with respect to the thruster on time.

Tables 10 and 11 report results for performing the GEO relocation of the servicer without and with the client, respectively, for a phasing angle of 90 deg with various propulsion system options. Specifically, the phasing angle is calculated as the difference between the client and the servicer true anomaly; thus, the servicer chases the client. A 90 deg phasing angle relocation is generally an onerous maneuver in terms of

required propellant mass, and this analysis aims to test the system for a challenging scenario. Furthermore, for low-thrust systems, time of flight is prioritized over propellant mass, and no coasting is performed. From the results reported in both Tables 10 and 11, we see that for both low-thrust and high-thrust maneuvers, the multimode system utilizes the most propellant, while the electric and chemical systems utilize the least propellant (for low-thrust and high-thrust respectively). As before, these trends are tied to the specific impulse of the propulsion system options. These tables also show that among high-thrust systems, the thruster on time values are nearly identical. For low-thrust systems, the multimode system has the lowest thruster on time, and the electric system has the highest thruster on time. These trends are again due to the different thrust values produced by each of the systems. As expected, the maneuver time is lower for high-thrust systems than low-thrust systems. However, for the phasing without the client (Table 10), all low-thrust systems are able to perform time-comparable maneuvers with respect to the high-thrust options using a fraction of the propellant mass. High-thrust systems could perform faster phasing maneuvers decreasing the number of coasting orbits at the expense of an already high propellant budget. In the case of client relocation (Table 11), the maneuver time for high-thrust systems is about half that of low-thrust systems. Additionally, for both Tables 10 and 11, maneuver time is significantly greater than the thruster on time for high-thrust systems and is comparable to the thruster on time for low-thrust systems. The ΔV for this maneuver is nearly identical for high-thrust systems, and varies a small amount for the low-thrust systems. Among the low-thrust systems, the multimode system has the highest ΔV, and the electric system has the lowest ΔV, with about 11 m/s and 7 m/s difference between the two systems for the phasing maneuver without and with the client, respectively.

Table 10: GEO Servicer Phasing Maneuver without Client for 90 deg Phasing Angle

Propulsion Mode	**Propellant Used**	**Thruster On Time**	**Maneuver Time**	ΔV
Chemical	39.02 kg	12.44 min	15.77 days	97.62 m/s
Electric	2.66 kg	18.98 days	20.49 days	52.25 m/s
Multimode High-Thrust	43.07 kg	12.41 min	15.77 days	97.63 m/s
Multimode Low-Thrust	6.74 kg	15.35 days	16.69 days	66.34 m/s
Hybrid High-Thrust	42.35 kg	12.42 min	15.77 days	97.63 m/s
Hybrid Low-Thrust	4.13 kg	16.5 days	18.17 days	60.89 m/s

Table 11: GEO Servicer Phasing Maneuver with Client for 90 deg Phasing Angle

Propulsion Mode	**Propellant Used**	**Thruster On Time**	**Maneuver Time**	ΔV
Chemical	136.58 kg	43.54 min	15.79 days	97.62 m/s
Electric	4.97 kg	36.07 days	37.7 days	27.88 m/s
Multimode High-Thrust	150.77 kg	43.45 min	15.78 days	97.62 m/s
Multimode Low-Thrust	12.37 kg	28.68 days	29.88 days	34.73 m/s
Hybrid High-Thrust	148.21 kg	43.47 min	15.79 days	97.62 m/s
Hybrid Low-Thrust	7.73 kg	31.41 days	32.70 days	32.53 m/s

Combination of Orbit Lowering and Phasing Maneuvers

A combined lower and phasing maneuver can also be performed. This maneuver involves the servicer starting in GYO, 90 deg out of phase with the client. Through three separate maneuvers, the servicer uses the high-thrust mode to lower its orbit to the client orbit (GEO) and change phase by 90 deg. The first maneuver is to lower the periapsis of the servicer such that its periapsis is equal to the client orbit radius. The servicer then moves on this "intermediate" orbit towards periapsis. The second maneuver occurs near periapsis and is an apoapsis-raise ΔV to increase the semimajor axis for coasting. The necessary semimajor axis and eccentricity of the coasting orbit are calculated based on the number of coasting orbits chosen. The simulation is set up such that the time taken for the client to move n coasting orbits ± 90 deg is equal to the time taken for the servicer to complete the transfer along the intermediate orbit$+(n-1)$ coasting orbits. The servicer is then propagated on the coasting orbit for approximately $n-1$ phasing orbits, until the servicer is close to periapsis. It is here that the servicer performs the final ΔV to lower the apoapsis, such that the servicer is in a circular orbit at the GEO altitude, now in-phase with the client. A diagram showing the combined lower and phasing maneuver using a high-thrust mode is shown in Fig. 10.

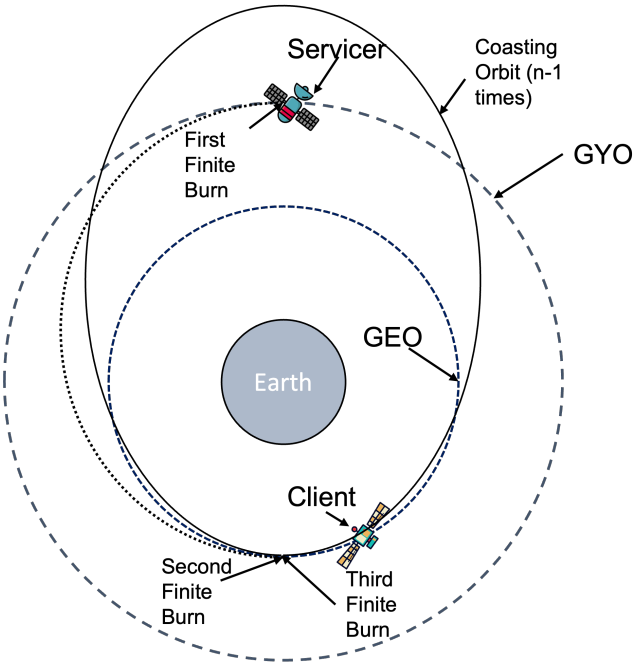

Figure 10: Combined lower and phasing maneuver using high-thrust mode.

A similar scheme can be used for the low-thrust maneuver. In this case, however, the servicer performs an active coasting phase, in which the thruster is first used to raise the servicer orbit and then lower the orbit to the client. Raising the orbit of the servicer increases the angular rate difference between servicer and client and reduces the coasting phase. The lower maneuver starts when the remaining phasing angle is equal to ϕ_{lower}, the phasing angle cancelled out during the lower maneuver. The coasting phase scheme is defined such that $\phi_{coast} = \phi_{coastUP} + \phi_{coastDOWN} = \phi - \phi_{lower}$ and $\phi_{coastUP} = \phi_{coastDOWN}$. The pre-phase of the maneuver could also be accomplished through a passive coasting maneuver, in which the servicer would wait GYO until the phasing angle is reduced to ϕ_{lower}. While a passive coast maneuver would enable the minimization of the required

Table 12: GEO Servicer Phasing Maneuver for Combined 90 deg Phasing Angle and Lower to GEO

Propulsion Mode	Propellant Used	Thruster On Time	Maneuver Time	ΔV
Chemical	41.47 kg	6.68 min	15.55 days	103.87 m/s
Electric	4.28 kg	30.23 days	35.68 days	84.15 m/s
Multimode High-Thrust	45.77 kg	6.7 min	15.54 days	103.87 m/s
Multimode Low-Thrust	10.61 kg	24.11 days	29.93 days	104.64 m/s
Hybrid High-Thrust	44.99 kg	6.67 min	15.55 days	103.87 m/s
Hybrid Low-Thrust	6.53 kg	25.98 days	32.44 days	96.41 m/s

propellant, it would also require a longer coasting time for a range of initial phasing angles. The active coasting maneuver allows faster phasing to the detriment of a slight increase in propellant usage. A diagram showing the combined lower and phasing maneuver using a low-thrust mode is shown in Fig. 11.

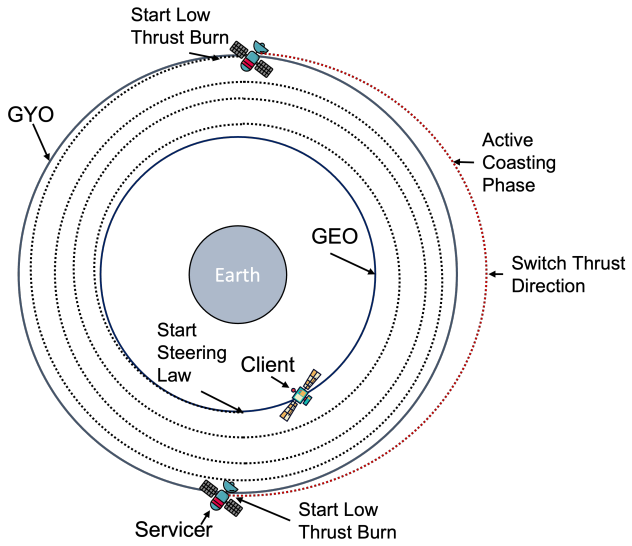

Figure 11: Combined lower and phasing maneuver using low-thrust mode.

Table 12 reports results for performing the combined GEO lower and phasing maneuver for a phasing angle of 90 deg with various propulsion system options. As before, the phasing angle is evaluated as the difference between the client and the servicer true anomaly. These results show similar trends as before in terms of the multimode systems requiring the largest amount of propellant among high- and low-thrust systems, respectively. Although the high-thrust systems tend to allow this combined phasing and lower maneuver to be performed in half the time of the low-thrust systems, the high-thrust systems require a significantly higher amount of propellant to complete the maneuver. In particular, the ratios of propellant required in the high-thrust mode to that required for the low-thrust mode are 4.31 and 6.89, for the multimode and hybrid systems, respectively.

LEO Maneuver Modeling

The LEO scenarios involve a client in a 53 deg inclination, 550 km circular orbit above the Earth. The servicer is initially in a perch orbit 50 km above the client, i.e. 600 km above the Earth. Maneuvers of interest include the servicer lowering and raising its orbit between the client and perch orbit, as well as changing phase with the client. A combined phasing and orbit raise/lower can also be performed. Spacecraft in LEO typically experience a portion of each orbit in eclipse, preventing solar panels from receiving energy. This effect has been considered for the low-thrust propulsion systems; for this reason, electric propulsion thrusters were considered unusable when in eclipse.

In this case, a symmetric thrust scheme was developed. The electric propulsion system remains off both during the eclipse and while passing through the region encompassing the symmetrical eclipse longitudinal angles with respect to the perpendicular to the Sun vector passing, as shown in Fig. 12 by the orange region. For the rest of the angles (green shaded region in the figure), the propulsion system thrust vector is assumed to be parallel to the inertial velocity vector. This thrust scheme enables an isotropic growth/decrease of the orbit (eccentricity $\simeq 0$); without the use of the symmetric thrust scheme nor any other steering control laws, the servicer orbit would increase/decrease in the direction of the Sun vector (eccentricity > 0).

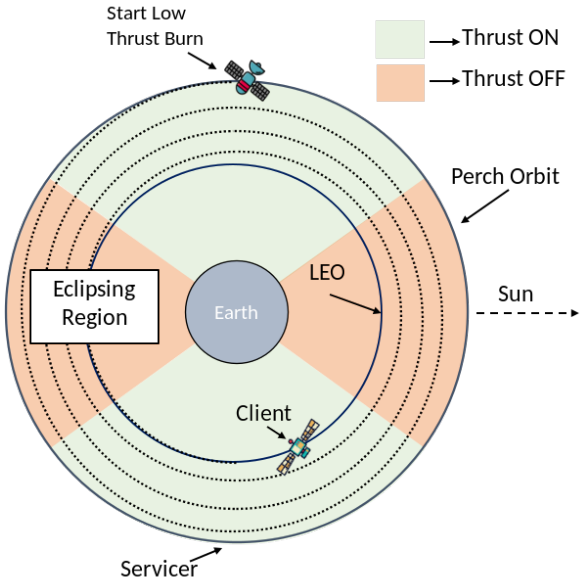

Figure 12: LEO lower with low-thrust mode accounting for eclipse

Perch Raise/Lower Maneuver

The perch raise/lower is the analog of the GYO raise/lower performed by the GEO servicers. As with the GYO raise, high-thrust (chemical) systems are simulated using two finite burns-one at periapsis and one at apoapsis. Also, similar to GEO, low-thrust systems utilize the symmetric thrust scheme, where the orbit altitude slowly increases over several revolutions. The thrust vector is assumed to be parallel to the inertial velocity vector for both the high- and low-thrust maneuvers.

Results for performing the LEO perch raise with various propulsion system options are shown in Tables 13 and 14 for maneuvers without and with the client, respectively. These results show that for high-thrust options, the chemical system utilizes the least propellant, while the multimode utilizes the largest propellant. For low-thrust options, the electric

system utilizes the least propellant, and the multimode system utilizes the most propellant. The raise with the client requires about 3-4 times as much propellant mass as a result of the added mass of the client. As with GEO, these trends are tied to the specific impulse of a given propulsion system. The thruster on time is nearly the same for all high-thrust options (among the raises with and without the client), but differs for low-thrust. The time taken for the low-thrust maneuvers relates to the amount of thrust each of the propulsion systems can provide and results in the multimode system having a thruster on time less than half that of the fully electrical system. The maneuver time for high-thrust systems is greater than the thruster on time but still on the order of minutes (half an orbital period in LEO). The maneuver time increases to the order of a half or full month for cases without the client and several months for the cases with the client. In general the thruster on time and maneuver time for the raises with the client are higher than for the cases without the client. The higher thrust magnitude of the multimode system pays off when considered eclipse; the multimode low-thrust system without the client is able to complete the maneuver in 15 days with respect to the 25 days of the low-thrust hybrid system and 35 days of the electric servicer, at the expense of a slight increase in the required propellant mass. The ΔV for this maneuver is nearly identical for all the propulsion system options.

Table 13: LEO Servicer Perch Raise Performance

Propulsion Mode	**Propellant Used**	**Thruster On Time**	**Maneuver Time**	ΔV
Chemical	1.1 kg	211.0 s	50.7 min	27.2 m/s
Electric	0.14 kg	22.29 days	34.67 days	27.48 m/s
Multimode High-Thrust	1.22 kg	211 s	56.73 min	27.21 m/s
Multimode Low-Thrust	0.28 kg	9.56 days	14.63 days	27.18 m/s
Hybrid High-Thrust	1.2 kg	211 s	56.73 min	27.21 m/s
Hybrid Low-Thrust	0.18 kg	16.7 days	25.55 days	27.19 m/s

Table 14: LEO Servicer Perch Raise Performance with Client

Propulsion Mode	**Propellant Used**	**Thruster On Time**	**Maneuver Time**	ΔV
Chemical	3.61 kg	690.54 s	62.71 min	27.22 m/s
Electric	0.46 kg	77.29 days	118.33 days	27.61 m/s
Multimode High-Thrust	3.99 kg	690.14 s	62.7 min	27.22 m/s
Multimode Low-Thrust	0.91 kg	32.06 days	49.06 days	27.33 m/s
Hybrid High-Thrust	3.92 kg	690.321 s	62.7 min	27.2 m/s
Hybrid Low-Thrust	0.6 kg	57.24 days	87.64 days	27.02 m/s

Phasing Maneuver

The phasing maneuver in LEO is similar to the phasing maneuver for the GEO servicers. For this analysis, high-thrust (chemical) systems are simulated using two maneuvers and 40 coasting orbits. Also, similar to GEO, low-thrust systems utilize a continuous-thrust-coast-thrust scheme, but this time, use the symmetric thrust scheme to prevent errors due to time in eclipse. The thrust vector is assumed to be parallel to the local velocity vector for both the high- and low-thrust maneuvers.

Tables 15 and 16 report results for performing the LEO phasing maneuver for a phasing angle of 90 deg with various propulsion system options without and with the client, respectively. For low-thrust systems, mission time has been prioritized, and no coasting is performed. These results show similar trends to before, with the propellant utilized and thruster on time dependent on the specific impulse and thrust magnitude, respectively. While the thruster on time itself is different orders of magnitude (minutes vs days) for high- and low-thrust systems, the total maneuver time is a similar order of magnitude between the two systems. However, due to the inclusion of the eclipse, low-thrust systems require longer maneuver time than high-thrust systems. From the results in Table 15, the mission time can very by a maximum of 13 days (i.e., electric servicer vs chemical servicer), this increase spikes up to 25 days for the phasing with the client case (Table 16). Also, the difference in propellant budget has a similar, but opposite trend, passing from a maximum decrease of approximately 4 kg (i.e., multimode high-thrust servicer vs electric servicer) for the phasing without the client case to a maximum decrease of approximately 13.3 kg for the phasing with the client. Overall, the multimode low-thrust as the best compromise between manevuer time and propellant used.

Table 15: LEO Servicer Phasing Maneuver without Client for 90 deg Phasing Angle

Propulsion Mode	**Propellant Used**	**Thruster On Time**	**Maneuver Time**	ΔV
Chemical	3.73 kg	11.9 min	2.71 days	93.33 m/s
Electric	0.06 kg	14.5 days	15.67 days	11.77 m/s
Multimode High-Thrust	4.11 kg	11.85 min	2.72 days	93.05 m/s
Multimode Low-Thrust	0.17 kg	9.59 days	10.81 days	16.7 m/s
Hybrid High-Thrust	4.04 kg	11.85 min	2.72 days	93.04 m/s
Hybrid Low-Thrust	0.09 kg	12.58 days	13.75 days	13.24 m/s

Table 16: LEO Servicer Phasing Maneuver with Client for 90 deg Phasing Angle

Propulsion Mode	**Propellant Used**	**Thruster On Time**	**Maneuver Time**	ΔV
Chemical	12.22 kg	38.97 min	2.73 days	93.4 m/s
Electric	0.1 kg	26.20 days	27.37 days	6.08 m/s
Multimode High-Thrust	13.47 kg	38.85 min	2.73 days	93.33 m/s
Multimode Low-Thrust	0.31 kg	17.22 days	18.41 days	9.3 m/s
Hybrid High-Thrust	13.27 kg	38.94 min	2.73 days	93.47 m/s
Hybrid Low-Thrust	0.16 kg	22.74 days	23.91 days	7.2 m/s

Combined Orbit Lowering and Phasing

A combined lower and phasing maneuver for the LEO case is similar to that examined for the GEO servicers. Like the GEO analysis, the high-thrust (chemical) systems for the LEO servicers are simulated performing a combined lower and 90 deg phasing maneuver using a set of three maneuvers. As before, the first ΔV lowers the periapsis to the client orbit, the second raises the apoapsis for coasting, and the third lowers the apoapsis to the client orbit.

Also, similar to GEO, low-thrust systems utilize a continuous-coast-thrust scheme, but in this case, use the symmetric thrust scheme to prevent errors due to eclipse. However, due to the higher angular speeds associated with LEO, the active coasting phase does not improve or speed up the maneuver as in GEO. For this reason, in LEO, a passive coasting phase is used, where the spacecraft coasts for a

predetermined time prior to performing a lower maneuver. This means that the lower maneuver starts when the phasing angle is equal to ϕ_{lower}, which is the phasing angle cancelled out during the lower maneuver. The coasting time is defined such that $\phi_{coast} = \phi - \phi_{lower}$. This approach enables the minimization of the required propellant. A diagram showing the combined lower and phasing maneuver using a low-thrust mode with passive coasting phase is shown in Fig. 13.

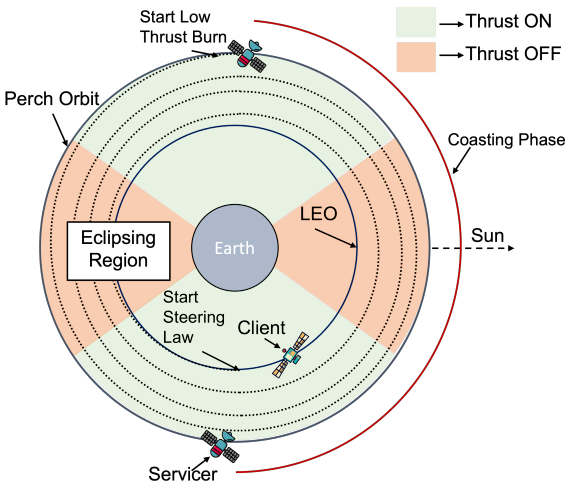

Figure 13: Combined lower and phasing maneuver using passive coasting phase in low-thrust mode for LEO.

Furthermore, Table 17 reports results for performing the combined phasing and lower maneuver in LEO for a phasing angle of 90 deg with various propulsion system options. As before, the multimode servicer performs the maneuver using the largest amount of propellant with respect to the same-thrust competitors. Also, the thruster on time is on the order of minutes for high-thrust systems and is on the order of days for the low-thrust systems. Furthermore, the maneuver time increases from 2 days for high-thrust systems to a month for low-thrust systems. The multimode low-thrust servicer is able to complete the maneuver in the fastest time (18 days) with respect to the same thrust mode competitors, with a small increase in the utilized propellant mass. Finally, the ΔV achieved with the proposed maneuver scheme for the high-thrust systems is about three times higher the ΔV achieved by the low-thrust systems.

Table 17: LEO Servicer Phasing Maneuver for Combined 90 deg Phasing Angle and Lower to LEO

Propulsion Mode	**Propellant Used**	**Thruster On Time**	**Maneuver Time**	ΔV
Chemical	3.79 kg	6.1 min	2.69 days	94.76 m/s
Electric	0.14 kg	22.66 days	40.74 days	27.49 m/s
Multimode High-Thrust	4.63 kg	6.74 min	2.69 days	94.61 m/s
Multimode Low-Thrust	0.28 kg	9.59 days	18.26 days	27.5 m/s
Hybrid High-Thrust	4.1 kg	6.08 min	2.7 days	94.68 m/s
Hybrid Low-Thrust	0.18 kg	16.9 days	30.11 days	26.93 m/s

4. Sensitivity Study

Propulsion System Parameters

We investigate variations in propulsion system parameters such as specific impulse, thrust magnitude, and propulsion system dry mass of the current system designs. The aim of this study is to determine how varying these parameters affect the overall performance of a system with respect to the current design point. The current multimode parameter values represent the modified theoretical values presented by Berg and Rovey [3] to account for losses in performance at a small scale, as well as achieve a higher flow rate in electrospray mode [16]. Given that system testing is ongoing, further variations in values are expected. Because variations in parameters are expected to not exceed $\pm 10\%$ from the current design, $\pm 10\%$ is set as the maximum offset magnitude for this study, and it is applied to all four systems.

The LEO and GEO thruster parameters detailed in this paper were varied, and the total ΔV capability of each system is calculated using the ideal rocket equation:

$$\Delta V = I_{sp} g \ln \left(\frac{m_{tot}}{m_{dry}} \right) \tag{8}$$

where m_{tot} is the total mass of the servicer and m_{dry} is the dry mass of the servicer. Equation (8) provides a good approximation of the available ΔV for a given propulsion system since the thrust angles are typically near zero (i.e. perpendicular to gravity). For the hybrid and multimode systems, a range of ΔV values are expected. The bounds of ΔV for hybrid represents the propellant usage that produces the highest and lowest amounts of ΔV: for the higher bound, all the chemical propellant available is expended first, followed by all the electric propellant, while the opposite occurs for the lower bound. Because all propellant is available to either thruster on the multimode system, the highest ΔV bound for multimode represents using only low-thrust propellant, while the lowest ΔV bound represent using only high-thrust propellant. Finally, any ΔV value within the hybrid and multimode bounds is possible, depending on the sequence of modes selected and indicates the degree of flexibility available for mission planning once the spacecraft is in orbit. Figure 14 displays variations of the specific impulse (I_{sp}), thrust, and propulsion system mass for the LEO thruster, while Fig. 15 displays these variations for the GEO thruster. The current design point is shown as a diamond marker.

Given that ΔV is an indicator of a spacecraft's lifetime and maneuver capability, as the ΔV increases, so does the number of missions a servicer can perform in orbit. As expected, when a system has a high specific impulse, it also has a high ΔV, hence a greater mission capability. Varying thrust has no effect on mission capability, and as the mass of the system decreases, the total ΔV increases, with a smaller impact. It is apparent that capability is more sensitive to variations in I_{sp}. While the specific impulse of state-of-the-art thrusters is not expected to vary significantly, differences in the multimode thruster parameters from the current design point are expected and could significantly impact the capability of the servicer. For LEO scenarios, improvements of 10% in the specific impulse of the multimode thruster could lead to an increase of about 50 m/s and 260 m/s of ΔV for the high- and low-thrust modes, respectively. Similarly, for GEO scenarios, improvements of 10% in the specific impulse of

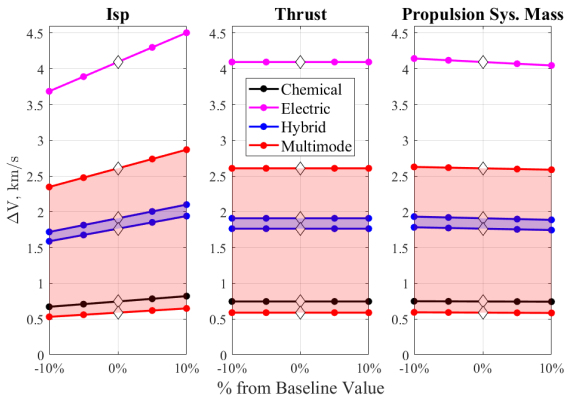

Figure 14: LEO Thruster Parameters Sensitivity Study.

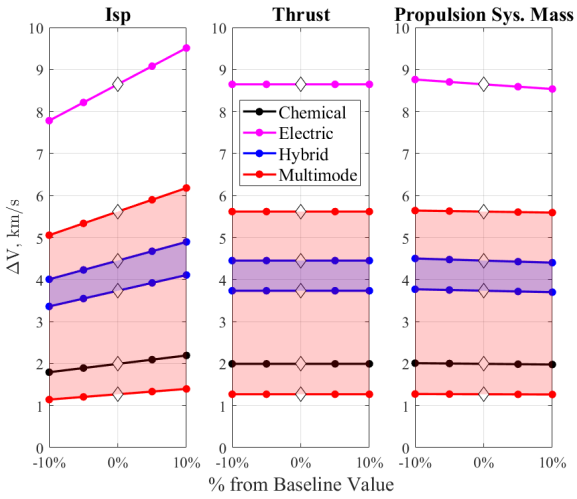

Figure 15: GEO Thruster Parameters Sensitivity Study.

the multimode thruster could lead to an increase of about 560 m/s and 125 m/s of ΔV for the high- and low-thrust modes, respectively.

Throughout the servicer's lifetime, one type of propulsion mode, or perhaps a combination of the two, may be optimal to accomplish a servicing request. This system feature is referred to as mission flexibility. Therefore, hybrid and multimode systems offer mission flexibility, which is quantified in the Figs. 14 and 15 by the area between ΔV bounds. Multimode and Hybrid systems are capable of any ΔV in their respective areas, but the multimode area is greater than the hybrid's for the entire study. Thus, Multimode offers a greater mission flexibility than the hybrid system for the servicing scenarios investigated.

Structural Coefficient Sensitivity Study

With the goal of optimizing mission lifetime and maneuver capability early in the design process, a sensitivity study in terms of structural coefficient was performed. The structural coefficient is expressed by the relation:

$$\sigma = \frac{m_S}{m_S + m_P} \tag{9}$$

where m_S is the structural mass (propulsion system dry mass, including thrusters, tanks, etc.), and m_P is the propellant mass.

The structural coefficient is an indicator of the efficiency of the propulsion system design and can be reformulated to depend on ΔV. ΔV is a metric of mission lifetime and maneuver capability. A high ΔV value indicates a high mission lifetime, meaning that more maneuvers can be performed with the available propellant. In contrast, a low structural coefficient indicates an efficient propulsive system design.

This study analyzes how the structural coefficient of the current GEO servicer with different propulsion systems varies with the ΔV possible and how the current sizing performs with respect to other potential designs for the specific system. ΔV is evaluated through Equation 8, where m_{tot} is equal to 1000 kg. The chemical and electric servicers have a unique ΔV, while hybrid and multimode present a range of ΔV. For the multimode servicer, the boundaries of the ΔV range are evaluated assuming that all the propellant mass is consumed with the high-thrust mode or low-thrust mode. The hybrid servicer range, however, cannot be evaluated as the multimode range because the hybrid servicer utilizes two different types of fuel on-board. In this case, the highest boundary is calculated assuming that all the chemical propellant is depleted first, followed by the he electric propellant. The lowest boundary is calculated under the assumption that the electric fuel is depleted first and then the chemical propellant.

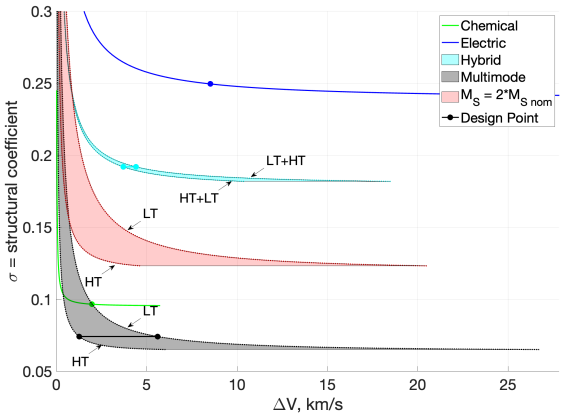

Figure 16: Structural coefficients variations for the four analyzed servicer in terms of budget.

Figure 16 show the result of this analysis. In the figure, the structural coefficients of the multimode and hybrid servicers are shown as bounded regions since these two servicers can use either the high-thrust/low I_{sp} system or the low-thrust/high I_{sp} system. This means that the servicer has a range of ΔV budget for any structural coefficient, which corresponds to any point on the horizontal line connecting the two bounds. Additionally, a longer length for the horizontal line indicates increased mission flexibility of the propulsion system. For the chemical and electric servicers, each structural coefficient instead corresponds to a specific ΔV budget due to their use of a single mode. The plot shows that the multimode system has a much greater ΔV range than the hybrid system.

Figure 16 also shows that the multimode servicer has the lowest structural coefficient for the same ΔV budget with

respect to the other servicers. This result is in line with the sizing results of Table 6, where it was shown that the multimode servicer has the lowest propulsion system dry mass. Furthermore, the current multimode design sits at about the optimal range of ΔV capability, indicating that the multimode design achieves extensive mission flexibility. The ΔV capability of the multimode outperforms the hybrid system capabilities.

This analysis also included a study of ΔV capability variation in the presence of structural mass uncertainty. The red region in Fig. 16 reports the multimode design if the propulsive system structural mass is doubled. Results show that doubling the propulsive system structural mass results in a higher structural coefficient and a slight decrease in ΔV capability; however, the multimode servicer still outperforms the hybrid servicer in terms of structural coefficient.

Structural Coefficient Variation throughout the Mission

The structural coefficient can also be evaluated as a function of the maneuver time or ΔV remaining. To this end, the structural coefficient changes in terms of the Δ V remaining during the mission as follows:

$$\begin{aligned}\sigma(t) &= \frac{m_S}{m_S + m_P(t)} \\ &= \frac{m_S}{m_S + m_{dry}\left[\exp\left(\frac{-\Delta V(t)}{I_{sp}g}\right) - 1\right]}\end{aligned} \tag{10}$$

where $\sigma(t)$ is the structural coefficient at time t, m_{dry} is the dry mass of the servicer, and $\Delta V(t)$ is the remaining ΔV budget at the time t.

Decreasing the remaining ΔV during the mission from its initial value (full propellant mass available) to zero (all propellant mass depleted) makes it possible to define the corresponding structural coefficient variation. Results of this analysis are shown in Fig. 17. Specifically, the plot reports the structural coefficient variation for all four servicers and the structural coefficient variation in the presence of structural mass uncertainties.

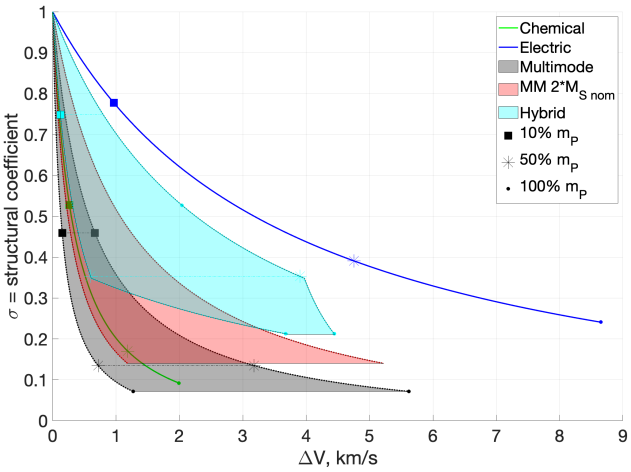

Figure 17: Structural coefficient variations in terms of ΔV for the four analyzed servicers.

In the plot, the structural coefficients corresponding to the beginning of the mission are the smallest values, with the largest ΔV (Dot marked points). The structural coefficients increase over the mission as remaining ΔV goes to zero, until reaching the value 1 ($\sigma = \frac{m_S}{m_S}$). Once again, both multimode and hybrid are represented by areas. In this case, the two boundaries of the multimode are found by fully depleting the propellant using either the high-thrust mode or the low-thrust mode. The hybrid servicer's lower-ΔV boundary is evaluated by first depleting all the chemical propellant and then the electric propellant. The higher-ΔV boundary is estimated by first depleting the electric propellant and then depleting the chemical propellant. For this reason, the hybrid servicer area is irregular.

Figure 17 also reports the structural coefficients for different values of remaining propellant mass: 100%, 50%, and 10%. These markers allow for a comparison between the servicer flexibility (ΔV range) and the efficiency of the design (σ) throughout the mission. The ΔV of the electric servicer is always the largest because of the high I_{sp} value of the thruster. The multimode initially shows the largest ΔV range, however this range shrinks as the remaining propellant decreases. For a fixed value of remaining propellant, the structural coefficient of the multimode is always the lowest.

Finally, Fig. 17 shows the multimode structural coefficient if the structural mass of the propulsion system is doubled. As the initial structural coefficient increases, the initial ΔV budget slightly decreases. Despite the large increase in propulsive structural mass, the multimode propulsion system outperforms both the electric and the hybrid systems.

5. Mission Performance

The maneuvers modelled with GMAT and discussed in Section 3 were combined and simulated to establish three distinct mission sequences: upgrade, relocation, and disposal of a client. For all sequences, the servicer begins in its loiter orbit, and performs a maneuver to lower to the targeted client, phasing accordingly. If the servicer is tasked to perform an upgrade sequence, a set amount of mass is transferred from the servicer to the client satellite, such as adding new payload into existing structural, electrical, or thermal interfaces to enhance the client's capabilities [2]. If the servicer is tasked to perform a relocation sequence, the servicer phases with the client and releases the client in its new desired slot. In the case of disposal, the servicer carries the client to its disposal orbit. After servicing, the servicer returns to its loiter orbit and maintains orbit for a set amount of time, until a new sequence is initiated.

The necessary individual maneuvers created in GMAT are run by a MATLAB script as indicated by the sequence being performed [14]. The states of the clients and servicers in question are gathered and updated from maneuver to maneuver and stored for analysis. To characterize the difference in performance between chemical, electric, hybrid, and multimode systems, the maneuver sequences are performed in cycles n times. Different propulsion types may be chosen to perform a cycle for hybrid and multimode propulsion. Mass and maneuver time are recorded for each system for analysis. If a system's maneuver capability is reached, meaning that there is not enough propellant to fulfill a sequence, the cycle stops, and the number of completed cycles is recorded.

Following the completion of each maneuver, the remaining

total impulse (I_{tot}) of each system is calculated. Total impulse is given by

$$I_{tot} = I_{sp} g_0 m_P \tag{11}$$

where m_P is the mass of the propellant left on-board the servicer. Similar to ΔV, total impulse is a metric of mission lifetime and maneuver capability: a high total impulse indicates a longer mission lifetime and capability. Total impulse does not vary with the servicer's dry mass, unlike ΔV, as it is only dependent on propellant mass. For hybrid and multimode systems, a range of total impulses is obtained by depleting all propellant available to different modes. The range is bounded by performing solely low-thrust and high-thrust sequences. For hybrid propulsion, total impulse bounds are given by

$$I_{tot} = I_{sp,c} g_0 m_{P,c} + I_{sp,e} g_0 m_{P,e} \tag{12}$$

where the subscript c represented high-thrust propulsion parameters, and subscript e represents low-thrust propulsion parameters. For multimode propulsion, total impulse is bounded by solely electric or solely chemical impulses rather than a combination of both.

Results are presented for four maneuver sequences simulated at GEO. First, an upgrade maneuver sequence to a client 90 deg away from the initial servicer position is simulated for $n = 6$ times. The amount of mass transferred with each sequence is 5 kilograms, and the servicer waits and maintains its orbit for 30 days following servicing. Orbit maintenance is performed in low-thrust mode, if propellant is available, to minimize the amount of fuel employed. Figure 18 displays the total impulse remaining of each system simulated with respect to the maneuver time left in the upgrade cycle. Next, the same upgrade maneuver sequence is repeated, however the serviced client is 45 deg away from the initial servicer position. Figure 19 displays the total remaining impulse of each system simulated with respect to the maneuver time left in this upgrade cycle.

Along with the upgrade maneuvers, a relocation maneuver of a client 90 deg away from the initial servicer position is simulated for $n = 10$ times. The client is relocated 90 deg from its initial state. Only low-thrust systems are capable of fulfilling this maneuver, and following relocation, the servicer raises back to GYO and maintains orbit for 30 days. Figure 20 displays the total remaining impulse of the low-thrust propulsion systems with respect to the maneuver time left in the relocation cycle. Finally, a disposal maneuver of a client 90 deg away from the initial servicer position is simulated for $n = 10$ times. After the servicer releases the client in its disposal orbit, it once again maintains orbit for 30 days until the next disposal maneuver. Figure 21 displays the total remaining impulse of the low-thrust propulsion systems with respect to the maneuver time left in the disposal cycle.

For each graph, the rightmost point of every line plotted represents the initial total impulse of a servicer, as well as the total time to complete the requested number of cycles. Across all simulations, electric propulsion holds the greatest total impulse, as well as the greatest amount of time to complete any cycle. The most notable variation in total impulse for any system is seen in performing the relocation sequence, as it demands the greatest amount of propellant out of all

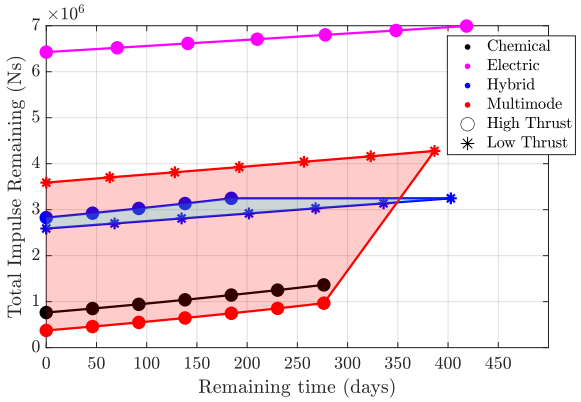

Figure 18: Total remaining impulse of all propulsion systems with respect to time left in mission cycle for upgrade sequence to a client 90 deg away

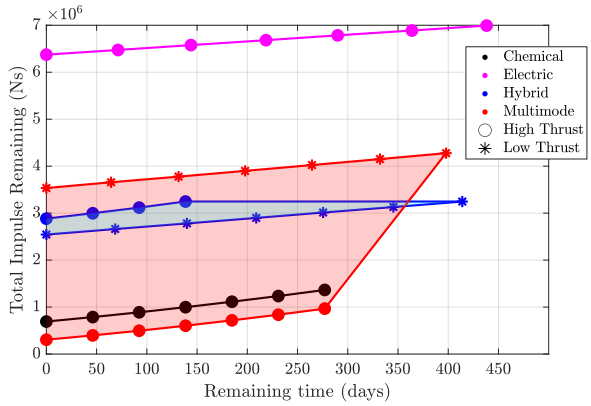

Figure 19: Total remaining impulse of all propulsion systems with respect to time left in mission cycle for upgrade sequence to a client 45 deg away

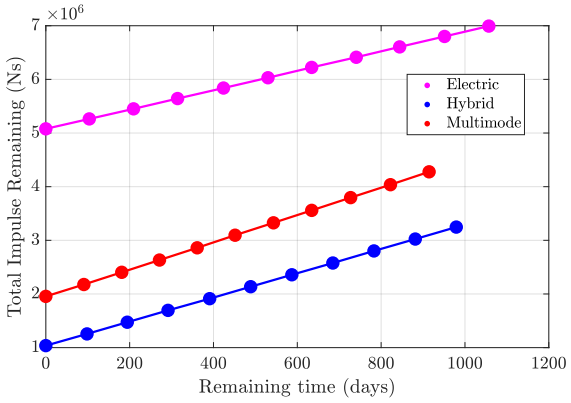

Figure 20: Total remaining impulse of low-thrust propulsion modes with respect to time left in mission cycle for relocation sequence

sequences. For the upgrade and disposal sequences, the areas bounded by high and low-thrust impulse lines of dual-mode systems represent all possible total impulses available at a certain time. In other words, the shaded areas represent the capability of multimode and hybrid system to perform maneuvers with different modes, also known as mission

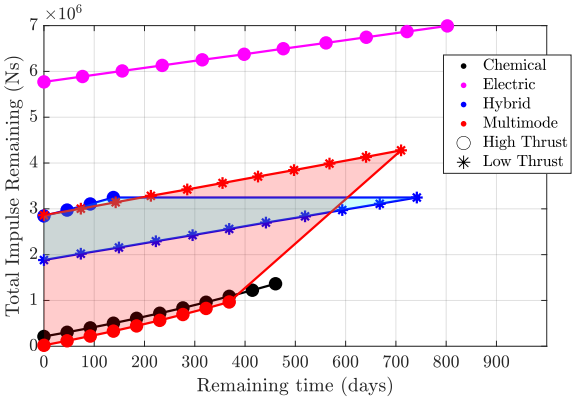

Figure 21: Total remaining impulse of all propulsion systems simulated with respect to time left in mission cycle for disposal sequence

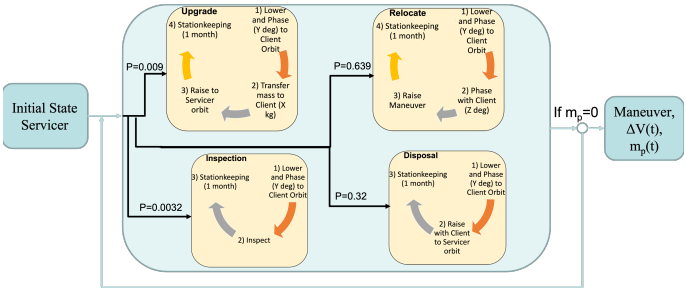

Figure 22: Flowchart for Markov chain mission sequence approach.

flexibility.

While solely chemical and electric systems appear to be highly performing systems compared to multimode and hybrid, they are restricted to a single mode of propulsion. Electric propulsion, while propellant efficient, is quite time intensive across all simulated cycles. Therefore, this system is not capable of fulfilling a high priority servicing request, potentially leading to the loss of clients. Alternatively, chemical propulsion is not propellant efficient but is less time intensive. Low maneuver capability means that chemical propulsion does not produce a lasting servicer capable of aiding clients on a long term basis. Multimode and hybrid systems are capable of fulfilling both high priority and long-term servicing needs. Furthermore, the multimode system consistently holds a greater mission flexibility than the hybrid system, as the multimode area of potential total impulses is larger than that of the hybrid system. This is a result of propellant pre-allocation on the hybrid system: because all propellant is available to both modes of propulsion, the multimode system's total impulse may be completely chemical and or electric, hence producing a wide range of impulses. In contrast, the hybrid system's propellant is pre-allocated to a specific mode; using all propellant available means combining low-thrust and high-thrust modes. Greater mission flexibility indicates that multimode propulsion will be able to access different modes of propulsion for a larger amount of servicing requests compared to hybrid. This is evident throughout most sequences simulated. In Figs. 18 and 19, the high-thrust mode of the hybrid system is not capable of fulfilling the 6 requested cycles, completing only 4 and 3 sequences respectively. Additionally, in Fig. 21, the high-thrust mode of the hybrid system can only fully complete 4 out of the requested 10 cycles, whereas high-thrust multimode can fully complete 8 cycles. Eventually, the high-thrust mode is not available to the hybrid servicer, and all remaining maneuvers must be performed as low-thrust time intensive maneuvers. Such behavior only occurs in the disposal sequence for the multimode servicer, as the same propellant is used for high- and low-thrust maneuvers.

Markov Chain Mission Sequence Model

A state machine approach is used to create random missions composed of a sequence of stochastic scenarios in a Markov Chain fashion, as shown in Fig. 22.

For this study, as visible from the flow chart, the scenarios simulated consist of Upgrade, Relocate, Disposal, and Investigate, as in the previous subsection. Each of these scenarios is composed of a sequence of maneuvers. For example, the Upgrade scenario consists of performing 1) a lower/phase combination maneuver to the client orbit, 2) a transfer of propellant mass to the client, 3) a raise maneuver to the GYO/perch orbit, and 4) station keeping for one month. The Relocate scenario is composed of 1) a lower/phase combination maneuver to the client orbit, 2) a phase with client maneuver, 3) a raise maneuver to the GYO/perch orbit, and 4) station keeping for one month. Next, the Disposal maneuver consists of 1) a lower/phase combination maneuver to the client orbit, 2) a raise maneuver to the GYO/perch orbit with the client, and 3) station keeping for one month. Lastly, the Investigation scenario consists of 1) a lower/phase combination maneuver to the client orbit, 2) a raise maneuver to the GYO/perch orbit, and 3) station keeping for one month.

All phasing angles and mass transfers were randomized to attempt to recreate a plausible multi-client environment. Thus, the servicer can phase a random angle between 1 and 359 deg and transfer a mass between 5 and 15 kg for the GEO case and between 0.5 and 1.5 kg for the LEO case. In this analysis, a sequence of scenarios is initially randomly defined. Although the sequence of scenarios is stochastic, the scenarios are chosen with different probabilities.

As mentioned previously, hybrid and multimode servicers can use both high-thrust and low-thrust to perform a maneuver. Generally, a low-thrust maneuver requires a low amount of propellant but a long maneuver time; for this reason, a low-thrust maneuver is preferable when time is not a constraint. However, to simulate criticality, the decision of performing a maneuver using a low-thrust or high-thrust thruster has been randomized when the servicer is called to reach the client (lower and phasing maneuver). Nevertheless, station keeping, raise to the GYO orbit, phasing with the client, and raise with the client always uses low-thrust mode when possible. Indeed, as shown in Tables 11 and 16 , the required propellant budget for the phasing with the client maneuver makes it prohibitive to be performed multiple times. Additionally, it is expected that the raise to GYO/perch orbit with or without the client would not be an urgent maneuver. Finally, we assume that if the chemical or the electric propellant has already been depleted, the hybrid servicer performs the maneuver using the mode with propellant available.

Once the mission sequence is fully defined, the four servicers perform their respective mission until the propellant mass is fully depleted. For each mission, mission time, ΔV remaining, and propellant consumed were tracked. The Markov

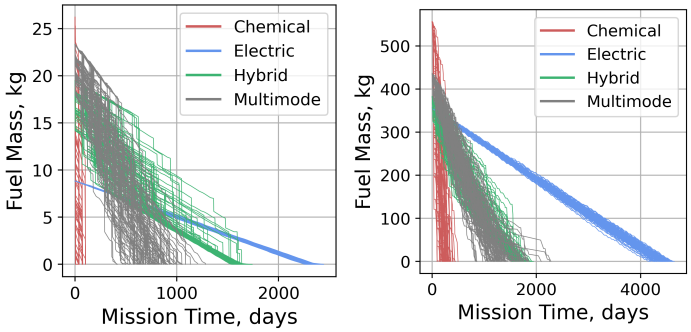

Figure 23: Fuel mass variations of 100 random missions for the four (a) LEO and the (b) GEO servicers.

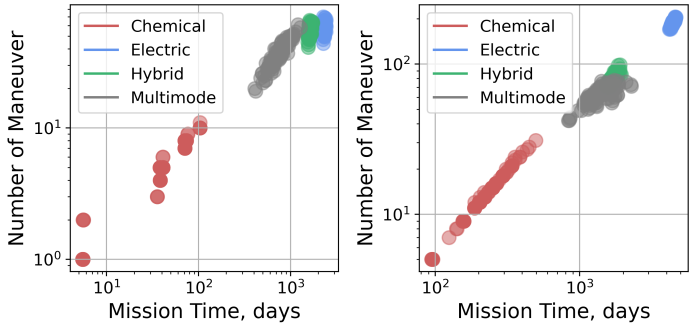

Figure 24: Total number of maneuvers and mission time for the 100 random missions for the (a) LEO and the (b) GEO servicers.

approach was used to simulate 100 random missions. The low-thrust mode was chosen with a probability of 0.5 for the hybrid and multimode systems to maintain extensive servicer capabilities along the mission.

Results of this analysis are presented in 23-27. All the results are presented both for the LEO and GEO cases. Specifically, Fig.23 shows the discrete fuel variations during the missions' progress. Generally, the LEO missions (Fig.23(a)) presents a shorter life-time than the GEO missions (Fig.23(a)). As an example, the majority of the multimode missions in LEO are completed in 1000 days, while in GEO these take around 2000 days. Also, the LEO servicers have a much lower initial propellant budget. Moreover, as visible from the plots, there are four defined trends both for the LEO and the GEO case; the chemical servicer depletes the fuel mass in the shortest time, and the overall slope of the chemical servicers curves results to be the sharpest. The electric servicer reports the shallowest slope resulting in the longest missions. Finally, hybrid and multimode servicers trends are not easily distinguishable, specifically for the GEO case; these two servicers tend to complete the missions in a comparable time and reports similar slopes. This results in comparable capabilities for the two servicers. For the LEO case, although the hybrid and multimode servicers trends are still not easily distinguishable, overall the multimode slope seems to be slightly steeper than the hybrid case.

The same conclusion can be inferred from Fig. 24, where the total final number of maneuvers is reported in the function of the final mission time. In these plots, it is visible how the four servicers show four distinct clusters both for the LEO (Fig. 24(a)) and the GEO (Fig. 24(b)) case. Indeed, chemical and electric servicers result clearly in the lowest and the highest number of maneuvers, respectively. Also, the hybrid and the multimode clusters overlap for the GEO case, while in LEO, the hybrid servicer performs a slightly higher number of maneuvers in longer time than the multimode cluster. Furthermore, from both plots, the hybrid servicer cluster results to have a lower variance with respect to the multimode cluster, which shows a larger variability between the number of maneuvers and total mission time along the 100 simulated missions. This is proof of a larger flexibility during the mission of the multimode servicer than the hybrid servicer with respect to the low- and high-thrust mode scheme used. Nevertheless, the hybrid and multimode exhibit similar performance and capabilities.

Furthermore, Fig. 25 shows the maximum ΔV budget in the

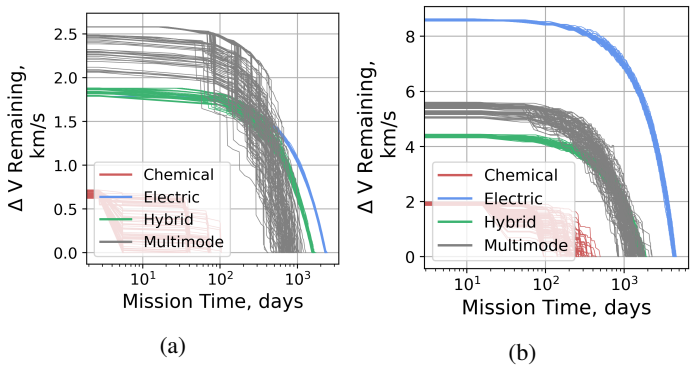

Figure 25: ΔV variation with respect to mission time for the four (a) LEO and the (b) GEO servicers.

function of the mission time. In this case, for the multimode servicer, the reported maximum ΔV corresponds to the low-thrust/high-I_{sp}; for the hybrid system, the maximum ΔV is the one corresponding to depleting all the chemical fuel first and then the electric fuel. For the LEO case shown in Fig. 25(a), chemical and multimode servicers report the lowest and the largest remaining ΔV, respectively. Instead, for the GEO case shown in Fig. 25(b), chemical and electric servicers report the lowest and the largest remaining ΔV, respectively. In LEO, the electric servicer is indeed able to allocate a smaller fraction of propellant with respect to the total system mass than in GEO because of the large propulsive system structural mass required. Multimode reports a larger initial ΔV with respect to the hybrid servicer in both LEO and GEO cases; this is in line with the previously presented results. However, this difference tends to shrink and overlap with time.

Figure 26 shows the average number of maneuvers performed during the missions and their standard deviation. Both plots of this figure specify the number of maneuvers performed using low- and high-thrust mode for the hybrid and multimode servicers. Once again, chemical and electric servicers report the lowest and highest number of maneuvers for both the LEO (Fig. 26(a)) and the GEO case (Fig. 26(b)). Also, multimode and hybrid servicers show comparable numbers of high-thrust maneuvers. In contrast, the hybrid servicer performs a slightly larger number of low-thrust maneuvers than the multimode case in GEO; this increase becomes more evident in the LEO case.

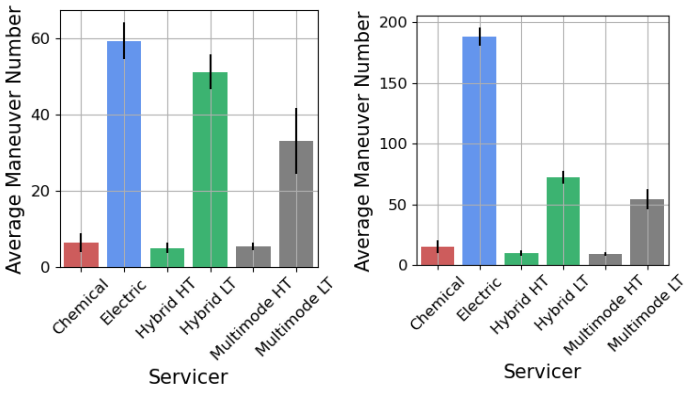

(a) (b)

Figure 26: Mean and standard deviation maneuver number for 100 random missions for the (a) LEO and the (b) GEO servicers.

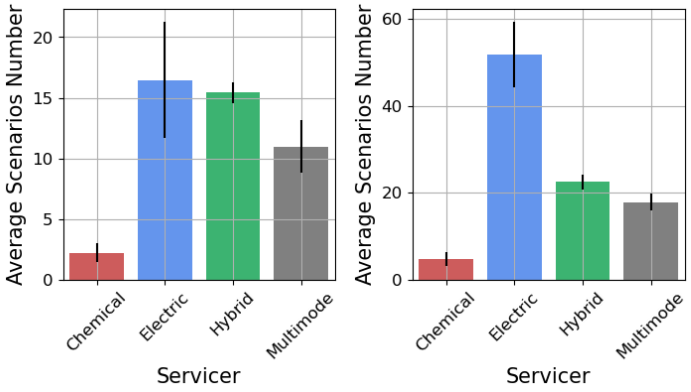

(a) (b)

Figure 27: Mean and standard deviation scenarios number for 100 random missions for the (a) LEO and the (b) GEO servicers.

Finally, Fig. 27 shows the average number of scenarios completed during the missions and their standard deviation. Also in this case, chemical and electric servicers report the lowest and highest number of scenarios for both the LEO (Fig. 27(a)) and the GEO case (Fig. 27(b)). Also in this case, the hybrid system is able to perform a slightly larger, but comparable, number of scenarios than the multimode case in both LEO and GEO orbits.

Overall, the results show that the electric servicer can perform more maneuvers more scenarios in a larger mission time both for the LEO and GEO servicers. However, an electric-only system does not allow for urgent, unplanned servicing maneuvers. Hybrid and multimode results show shorter mission times than the electric-only system and, relative to each other, similar capabilities from a mission performance perspective, also allowing for unplanned servicing maneuvers.

6. Conclusions

This paper analyzed a LEO servicer (with a total mass of 100 kg) and a GEO servicer (with a total mass of 1000) using the four different propulsive systems: chemical, electric, hybrid, and multimode. Propulsion system sizing routines were developed for the four propulsive system options. Results show that the multimode propulsion system has the lowest dry mass (4.11 kg and 48.55 kg lower than the hybrid servicer for LEO and GEO, respectively) and smaller pressurant tanks (0.61 and 0.59 times the radii of the fully electric system, for LEO and GEO, respectively) for both the LEO servicer and the GEO servicer. Additionally, the multimode sizing results the lowest structural coefficient for GEO (0.08), which indicates a mass-efficient propulsive system design, and the largest ΔV range (1.26-5.56 km/s), which enhances mission flexibility.

A set of likely servicer maneuvers were modeled, for both LEO and GEO orbits. Results show that the multimode servicer requires the largest amount of propellant for each maneuver, relative to other servicers performing the maneuver with the same mode (low- or high-thrust); this is due to the relatively low specific impulse values of the multimode servicer with respect to the other three options. Also, this analysis showed that phasing and raise maneuvers with the client require more propellant than offered by the high-thrust modes.

A sensitivity study on the thruster parameters for both LEO and GEO servicers (i.e. specific impulse, thrust and propulsion system mass) was performed. Results indicate that variations in specific impulse have the greatest impact on the servicer design. For LEO, improvements of 10% in specific impulse led to an increase of about 260 m/s and 50 m/s in low-thrust and high-thrust modes of the multimode servicer respectively, whereas the same improvements lead to an increase of about 560 m/s and 125 m/s for the GEO multimode servicers.

Upgrade, disposal, and relocation maneuvers were repeatedly simulated at GEO for a set number of times, and the performance of each system was analyzed. Notably, multimode offers a greater mission flexibility than hybrid system, as it may complete both propellant and time efficient servicing demands for a higher amount of maneuvers and longer mission lifetime compared to the hybrid system. Finally, randomized Markov Chain mission sequences were simulated to evaluate the servicer's performance in a plausible multi-client LEO and GEO environments. Overall, results show that while an electric servicer performs the largest number of maneuvers and can service the most clients, it does not allow for unplanned servicing maneuvers. Hybrid and multimode systems show comparable capabilities from a mission performance perspective, allowing also for unplanned servicing maneuvers. However, multimode has a much lower propulsive system dry mass and more efficient propulsive system design.

Acknowledgments

The research reported here was partially supported by the Defense Advanced Research Projects Agency Grant No.: HR00112110003. The content of this paper does not necessarily reflect the position or the policy of the Government, and no official endorsement should be inferred.

References

[1] W.-J. Li and et al., "On-orbit service (OOS) of spacecraft: A review of engineering developments," *Progress in Aerospace Sciences*, vol. 108, pp. 32–120, 2019.

[2] J. P. Davis, J. P. Mayberry, and J. P. Penn. On-orbit: Inspection, repair, refuel, upgrade, and assemply of satellites in space. [Online]. Available: https://aerospace.org/sites/default/files/2019-05/Davis-Mayberry-Penn_OOS_04242019.pdf

[3] S. P. Berg and J. L. Rovey, "Assessment of multimode spacecraft micropropulsion systems," *Journal of Spacecraft and Rockets*, vol. 54, no. 3, 2017.

[4] J. L. Rovey and et al., "Review of multimode space propulsion," *Progress in Aerospace Sciences*, vol. 118, no. 100627, 2020.

[5] C. T. Lyne, J. L. Rovey, and S. P. Berg, "Monopropellant-electrospray multimode thruster testing results: Electrospray mode," *AIAA Propulsion and Energy 2021 Forum*, 2021.

[6] M. D. Griffin and J. R. French, *Space Vehicle Design*, 2nd ed. Reston, VA: American Institute of Aeronautics and Astronautics, 2004.

[7] R. W. Humble, G. N. Henry, and W. J. Larson, *Space Propulsion Analysis and Design*. New York: McGraw-Hill, 1995.

[8] National library of medicine: Hydrazine. [Online]. Available: https://pubchem.ncbi.nlm.nih.gov/compound/Hydrazine

[9] Ariane group: Hydrazine propellant tanks. [Online]. Available: https://www.space-propulsion.com/spacecraft-propulsion/hydrazine-tanks/index.html

[10] J. R. Wertz, D. F. Everett, and J. J. Puschell, *Space mission engineering: the new SMAD*. Microcosm Press, 2011.

[11] NASA state of the art small spacecraft technology: In-space propulsion. [Online]. Available: https://www.nasa.gov/smallsat-institute/sst-soa-2020/in-space-propulsion

[12] Clyde space: Starbuck-mini. [Online]. Available: https://www.aac-clyde.space/assets/000/000/187/AAC_DataSheet_Starbuck-Mini_original.pdf?161427581

[13] M. Mirshams and E. Zabihian, "Fadsat: A system engineering tool for the conceptual design of geostationary earth orbit satellites platform," *Proceedings of the Institution of Mechanical Engineers, Part G: Journal of Aerospace Engineering*, vol. 233, no. 6, pp. 2152–2169, 2019.

[14] D. J. Conway and S. P. Hughes, "The general mission analysis tool (GMAT): Current features and adding custom functionality," *International Conference on Astrodynamics Tools and Techniques (ICATT)*, 2010.

[15] N. S. Gopinath and K. N. Srinivasamuthy, "Optimal low thrust transfer from gto to geosynchronous orbit and stationkeeping using electric propulsion system," *54th International Astronautical Congress of the International Astronautical Federation, the International Academy of Astronautics, and the International Institute of Space Law*, 2003.

[16] S. Berg and et al., "Electrospray of an energetic ionic liquid monopropellant for multi-mode micropropulsion applications," *51st AIAA/SAE/ASEE Joint Propulsion Conference*, 2015.

BIOGRAPHY

Giusy Falcone *is a Ph.D. candidate in the aerospace engineering department at the University of Illinois Urbana-Champaign. Her areas of expertise lie in hypersonic and space systems; space guidance, navigation, and control; flight mechanics; and mission design. Her research focuses on autonomous aerobraking technology development. She is one of the recipients of the Robert Beatty Fellowship, Mavis Future Faculty Fellowship, and the Aerospace Engineering Alumni Advisory Board Fellowship.*

Daniel Engel *is a graduate student in aerospace engineering in the Putnam Research Group at the University of Illinois Urbana-Champaign and a NASA space Technology Graduate Research Opportunities fellow. His research interests include space mission design and flight mechanics and guidance, navigation and control for planetary entry systems. He received is B.S. at the University of Illinois Urbana-Champaign as well.*

Marta Cortinovis *is an undergraduate student pursuing a B.S. in aerospace engineering at the University of Illinois Urbana-Champaign, where she is a member of the Putnam Research Group. Her research focuses on flight mechanics for aerobraking maneuvers, as well as mission analysis of multimode propulsion systems. She previously interned at Froberg Aerospace, supporting research efforts in multimode micropulsion thrusters and propellant synthesis. In 2021, she became a Barry Goldwater Scholar.*

Charles N. Ryan *is a lecturer (Assistant Professor) in Astronautics at the University of Southampton, United Kingdom. Dr. Charlie Ryan completed his Ph.D. in aerospace engineering in 2011 from Queen Mary University of London, investigating the fundamentals of the electrospray process. Dr. Charlie Ryan specialises in the experimental investigation of space propulsion for small satellites, in particular electrospray thrusters and green chemical propulsion.*

Joshua L. Rovey *Joshua L. Rovey received the Ph.D. degree in aerospace engineering from the University of Michigan, Ann Arbor, MI, USA, in 2006. He studied gridded ion thruster hollow cathode erosion. In 2017 he joined as a Faculty Member with the Department of Aerospace Engineering, University of Illinois Urbana-Champaign, Urbana, IL, USA where he leads the Electric Propulsion Laboratory. He has authored over 120 conference and journal publications in space propulsion and plasma studies.*

Zachary R. Putnam *is an assistant professor in the Department of Aerospace Engineering at the University of Illinois Urbana-Champaign. He leads a research group focused on mission design and analysis for hypersonic and space systems with a focus on guidance, navigation, and control. Dr. Putnam was previously a member of the technical staff at the Draper Laboratory. Dr. Putnam earned his Ph.D., M.S., and B.S. in aerospace engineering from the Georgia Institute of Technology.*

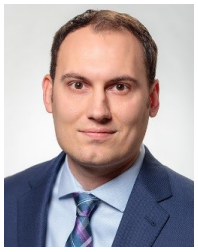

Steven Berg *is the CEO and co-founder of Froberg Aerospace, LLC, a company focused on the development of multimode spacecraft propulsion systems. Dr. Berg earned his PhD in Aerospace Engineering from the Missouri University of Science and Technology for his work in developing multimode capable ionic liquid propellants. As CEO of Froberg Aerospace, he has led development of the first multimode system to use the same propellant and same thruster head. He has previously been a propulsion and test engineer at SpaceX and is also currently a part-time lecturer in Aerospace Engineering at North Carolina State University.*

Michael Lembeck *(B.S. '80, M.S. '81, Ph.D., '91 UIUC) is a Clinical Associate Professor in the Aerospace Engineering Department at the University of Illinois Urbana-Champaign. He is also the Director of the Laboratory for Advanced Space Systems at Illinois providing students with opportunities to design, build, and fly experimental CubeSat satellites. Dr. Lembeck has 40 years of experience in commercial space, in government contracting, and as the Requirements Division Director for the Exploration Systems Mission Directorate at NASA Headquarters, he led the development of requirements for the original Constellation/Orion program.*